DETECTION OF COMBINE-HARVESTER FEED QUANTITY BASED ON MULTI-SOURCE INFORMATION FUSION

/

基于多信息融合的联合收割机喂入量检测方法研究

Jizhong WANG[1)*], Wei DONG[1)], Yong WU[2)], Yangchun LIU[3)], Hongze GUO[3)]

[1)] Weifang University, Weifang, 261061, China

[2)] Shandong Maritime Vocational College. Weifang, 261061, China

[3)] State Key Laboratory of Agricultural Equipment Technology,

China Academy of Agricultural Mechanization Science Group Co., Ltd. Beijing 100083, China

Tel: +86-13651380575; E-mail: 780227311@qq.com-

DOI: https://doi.org/10.35633/inmateh-79-38

Keywords: *combine harvester; information fusion; feed quantity; harvest loss; grey relational analysis*

ABSTRACT

This study proposes a real-time method for detecting combine-harvester feed quantity based on multi-source information fusion and error correction, with the aim of addressing control delays caused by information lag. Field tests were conducted to obtain key parameters, including feeding-auger torque and threshing-drum torque, determine their relational weights, and establish a prediction model. The model achieved a maximum relative error of 9.64% and a mean relative error of 4.55%, meeting the requirements of practical field operation.

摘要

本研究旨在提出一种基于多信息融合与误差修正的联合收割机喂入量实时检测方法，以解决信息滞后导致的控制延迟问题。通过田间试验获取喂入搅龙转矩和脱粒滚筒转矩等关键参数，确定其关联权重，并建立预测模型。模型检测最大相对误差 9.64%，平均相对误差 4.55%，可满足实际作业需求。

INTRODUCTION

Combine harvesters possess the capability to carry out integrated multi-harvesting operations that encompass the direct harvesting of grain from the field. To maximize operational efficiency, parameters such as the feed quantity of the harvester and the width of the header have been progressively increasing in recent years (*Mathanker et al., 2015; Jiang et al., 2025; Chen et al., 2019*). Nevertheless, achieving an effective match between the separation, cleaning capabilities, and feed quantity of the harvester remains a pressing concern in practical operations. This is due to the challenges posed by excessive grain loss and high impurity content during the operational process. Consequently, it holds great significance to investigate a precise and efficient method for predicting the feed quantity of harvesters (*Li et al., 2024; Sun et al., 2022; Zhang et al., 2025*), which would facilitate comprehensive performance control and harvest loss reduction (*Wang et al., 2026*). The feed quantity of the harvester is defined as the total mass of harvested crops that are conveyed to the harvester feeding auger per unit time. The feed quantity is a crucial performance parameter of harvesters during harvesting operations, as it reflects the overall performance of the operation (*Li et al., 2026; Liang et al., 2024; Zhang et al., 2024*). The performance of the harvester can be affected by an excessive or insufficient feed quantity (*Saeys et al., 2009; Zhang et al., 2022*). A larger feed quantity, for instance, may cause the harvester to become overloaded, thus diminishing the overall performance of the operation, while increasing the rate of grain loss and damage. Conversely, a smaller feed quantity can lead to a significant decrease in operational efficiency and an increase in entrainment loss during operation, resulting in a reduced overall performance of the harvester. Consequently, accurate detection of the feed quantity of the harvester is highly significant and merits attention (*Wang et al., 2023; Abdeen et al., 2022; Chen et al., 2025; Yang et al., 2025*).

Four main approaches are currently used to detect or estimate combine-harvester feed quantity. The first estimates feed quantity by directly measuring the grain flow rate within the harvester *(Liu et al., 2018; Sangeetha et al., 2024)*. The second predicts feed quantity from the power consumption of the threshing mechanism. The third combines real-time grain-flow measurements with threshing-drum power consumption to improve feed-quantity estimation. The fourth predicts feed quantity by monitoring the torque and compressive force of key harvester components during operation *(Fricke et al., 2011; Ebrahimi et al., 2009; Wang et al., 2026)*.

Firstly, the correlation weight is employed to scrutinize and define the correlation extent of every influential factor towards the forecasting of feed quantity. Subsequently, by scrutinizing the feed quantity time lag of the data samples procured from sensors that exert a significant impact on the indicators, a multi-information integration-based error correction technique is proposed to rectify the model. Finally, a field validation experiment is formulated and executed to authenticate the efficiency of the formulated feeding prediction model.

First, grey relational analysis was used to determine the relative influence of each factor on feed-quantity prediction. Next, the time delays in the sensor data associated with the parameters having the greatest influence on feed quantity were analyzed, and an error-correction method based on multi-source information fusion was developed to improve the prediction model. Finally, field-validation experiments were designed and conducted to evaluate the effectiveness of the proposed feed-quantity prediction model.

MATERIALS AND METHODS

Sample data acquisition test design

The field experiment was conducted at the wheat plantation base of Qingdao Jimo Shengfa Cooperative, using the GM series wheat combine harvesters of Lovol Geso as the experimental prototype. The experimental procedures were carried out in strict accordance with the national standard GB/T8097-2008 Equipment for Harvesting — Combine Harvesters — Test Procedure. According to this standard, the test plot was selected with a length of no less than 30 m and a width sufficient to accommodate the full working width of the header, ensuring stable and representative operating conditions. For each test run, the combine harvester was operated at a constant preset speed over a total distance of 30 m in a straight line. The first 10 m served as the preliminary acceleration and stabilization phase, during which no data were recorded. Once the harvester reached the steady operating state, data were collected over the remaining 20 m sampling distance. Each test condition was repeated three times, and the mean values of each parameter were used for subsequent analysis to minimize random experimental errors, as illustrated in Fig. 1.

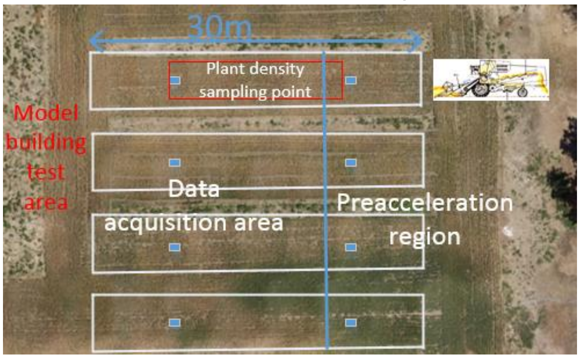

Fig. 1 - Schematic diagram of combine harvester field test scheme

Prior to the formal tests, a preliminary sampling survey of wheat crop properties was conducted within the test plot. Five representative 1 m × 1 m sampling areas were randomly selected to determine crop density, with the above-ground biomass harvested, oven-dried to constant weight at 105 °C, and weighed using an electronic balance (accuracy ±0.01 kg). The results indicated that the wheat had fully ripened, with a grain moisture content of 14.2% ± 0.5%, as measured by a grain moisture meter (PM-8188, Kett Electric Laboratory, Japan), which satisfied the harvesting standards specified in GB/T8097-2008. The test terrain was flat and the wheat growth was uniform with minimal weed presence, as illustrated in Fig. 2. These site conditions ensured the reliability and repeatability of the experimental data.

a) *b)*

Fig. 2 - Wheat growth and field test

a) Field harvesting operation scene; b) Field harvesting operation scene

In the sampling area, a mesh collection bag was securely attached to the rear of the harvester to collect all impurities and threshed straw discharged during operation. After the harvester completed a 20 m test run, the contents of the bag were removed, sorted, and weighed, and a portion was retained as samples for subsequent tests. Ten tests were conducted following this procedure. For each test, the mean value of each performance index was used as the dataset for the corresponding group, as shown in Table 1.

Table 1

Field test data of operation parameters of key components of combine harvester

No.	Average feeding Quantity (kg/s)	Harvest speed (m/s)	Feeding auger torque(Nm)	Feeding auger rotation speed (r/min)	Threshing drum torque (Nm)	Threshing drum rotation speed (r/min)	Fan speed (r/min)
1	0.98	0.48	4.35	140.56	22.53	671.09	890.21
2	2.29	0.79	13.64	180.98	48.97	930.87	902.37
3	2.61	1.06	15.21	204.73	45.38	972.01	1005.70
4	3.56	1.41	24.98	192.31	74.89	990.58	990.38
5	4.04	1.37	45.47	118.93	85.31	598.49	1156.10
6	5.21	1.84	38.96	150.96	140.92	776.87	1056.26
7	5.70	1.91	58.69	155.89	128.69	909.31	998.39
8	6.13	2.11	49.24	200.14	149.25	1021.34	1156.19
9	6.52	2.84	54.68	188.20	145.39	1100.52	1200.47
10	7.69	3.31	62.38	220.56	162.11	1245.36	1099.68

Analysis of the feed-quantity prediction model

Analysis of the relative influence of different factors

Feed quantity is affected by multiple operating parameters, and analyzing it on the basis of a single variable may introduce considerable uncertainty. Therefore, the grey relational weighting method was used to evaluate the relative influence of each factor on feed quantity and to clarify the effects of the different operating parameters. The procedure for determining the relational weights included establishing the reference sequence, normalizing the comparison sequences, calculating the relational coefficients between the reference and comparison sequences, and determining the grey relational grades. Feed quantity was selected as the reference sequence, while operating speed, feed-auger torque and rotational speed, and threshing-drum torque and rotational speed were used as the comparison sequences. The grey relational weighting method was then applied to determine the relative contribution of each factor to feed quantity, as shown in Fig. 3. The factors were ranked according to their relational weights as follows: harvester operating speed, 0.89; feeding auger torque, 0.84; and threshing drum torque, 0.72.

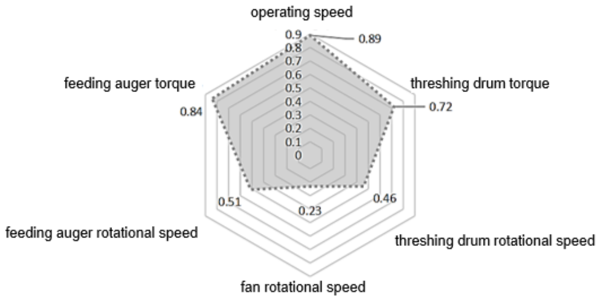

Fig. 3 - Influence weight of various factors on feed quantity

Analysis of the feed-quantity prediction model

Feed quantity is influenced not only by the operating parameters of the combine harvester but also by field crop characteristics, among which crop density is a key factor. To simplify the analysis and incorporate the measured crop-density data, crop density was divided into three categories: low, medium, and high. The corresponding ranges were 0.7~1.0kg/m^2, 1.0~1.3 kg/m^2, and 1.3~1.8 kg/m^2, respectively. By analyzing the relationship between the different crop-density ranges and feed quantity, a more accurate feed-quantity prediction model can be established.

Relationship between operating speed and feed quantity

Figure 4 presents the curve-fitting results based on the experimental data and shows the relationship between operating speed and feed quantity under low-, medium-, and high-crop-density conditions.

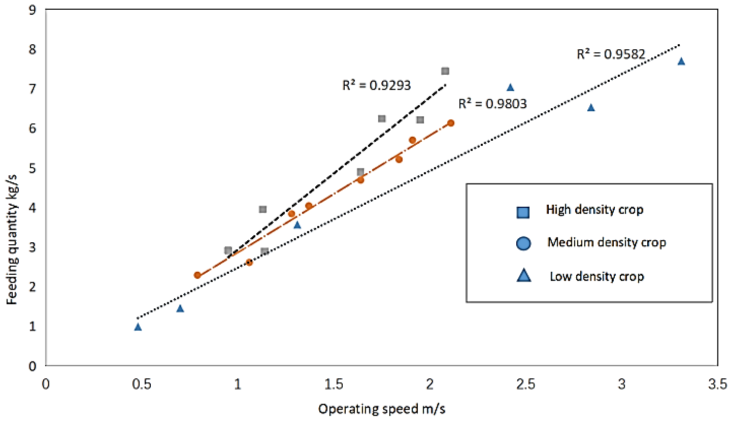

Fig. 4 - Regression curve between operating speed and feed quantity

The results shown in Fig. 4 indicate that, at the same operating speed, harvester feed quantity generally increased with crop density under low- and medium-speed conditions. However, under high-speed conditions, feed quantity was lower in the medium- and high-density crop regions than in the low-density crop region. To account for the combined effects of crop density and operating speed, their product was used as a composite influencing factor. A scatter plot describing the relationship between this factor and feed quantity is presented in Fig. 5.

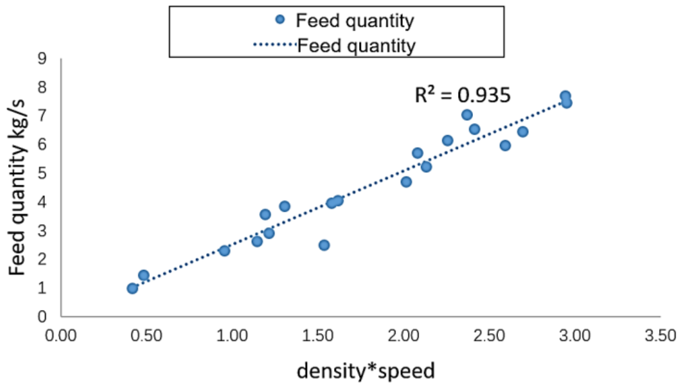

Fig. 5 - Regression relationship between the product of operating speed and wheat crop density and feed quantity

Table 2 presents the least-squares linear regression model for feed quantity, obtained by regressing harvester feed quantity against the product of operating speed and crop density.

Table 2

Regression relationship between the product of operating speed and wheat density and feed quantity

Model form	Regression equation	Coefficient of determination
y=a x+b	y=2.5668x+0.0632	0.935

Relationship between threshing-drum torque and feed quantity

Fig. 6 presents the curve-fitting results obtained from the experimental data and shows the relationship between threshing-drum torque and feed quantity under different crop-density conditions.

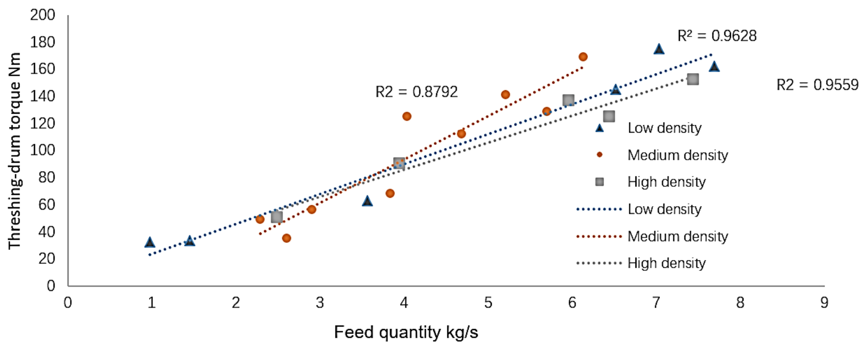

Fig. 6 - Relationship between threshing-drum torque and feed quantity under different crop-density conditions

As shown in Fig. 6, threshing-drum torque exhibited a strong linear relationship with feed quantity under low- and high-crop-density conditions. Under medium-crop-density conditions, the coefficient of determination was lower than those obtained for the other two density levels, although the linear relationship remained relatively strong. The corresponding regression models are presented in Table 3. These results indicate that a piecewise feed-quantity prediction model based on crop-density level is appropriate.

Table 3

Regression models relating feed quantity to threshing-drum torque under different crop-density conditions

Crop-density level	Model form	Regression equation	Coefficient of determination
Low density	y=a x+b	y=22.102x+34.83	0.9628
Medium density	y=a x+b	y=32.039x-34.837	0.8792
High density	y=a x+b	y=19.911x+34.83	0.9559

A multi-model regression analysis was conducted for the medium-crop-density condition to identify the most appropriate relationship between feed quantity and threshing-drum torque. The fitted models and their corresponding parameters are presented in Table 4, while the regression curves for the different model forms are shown in Fig. 7.

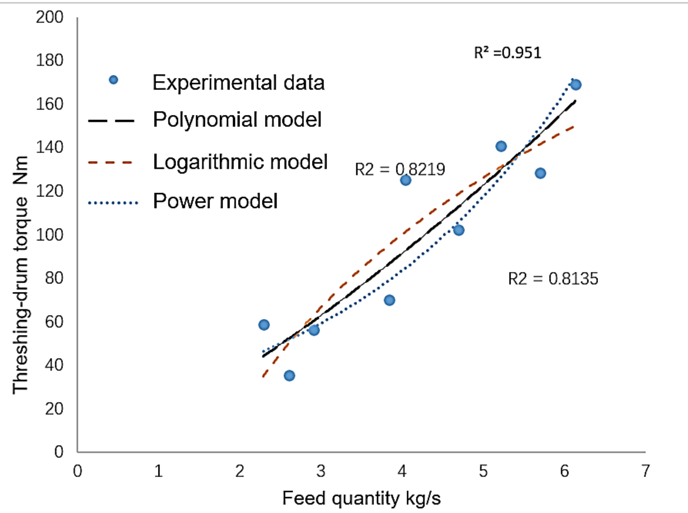

Fig. 7 - Regression curves relating feed quantity to threshing-drum torque using different model forms

As shown in Fig. 7, the quadratic model provided the best fit, with a higher coefficient of determination than the logarithmic and power models. Therefore, the quadratic model was selected to predict feed quantity under medium-crop-density conditions. The parameters and coefficients of determination of the fitted models are presented in Table 4.

Table 4

Comparison of regression models relating feed quantity to threshing-drum torque under medium-crop-density conditions

Crop-density level	Model form	Regression equation	Coefficient of determination
Low density	y=a x+b	y=22.102x+34.83	0.9628
Medium density	y=a x+b	y=32.039x-34.837	0.8792
High density	y=a x+b	y=19.911x+34.83	0.9559

In conclusion, linear regression models were suitable for describing the relationship between feed quantity and threshing-drum torque under low- and high-crop-density conditions, whereas a quadratic regression model was more appropriate under medium-crop-density conditions. The final piecewise prediction models are summarized in Table 5.

Table 5

Piecewise regression models relating feed quantity to threshing-drum torque

Crop-density level	Model form	Regression equation	Coefficient of determination
Low density	y=a x+b	y=22.102x+34.83	0.9628
Medium density	y=ax2+bx+c	y=1.3429x2+19.212x -6.7705	0.951
High density	y=a x+b	y=19.911x+34.83	0.9559

Analysis of the relationship between feeding-auger torque and feed quantity

Based on the experimental data, scatter plots were generated to illustrate the relationship between feeding-auger torque and feed quantity under different crop-density conditions. Regression analysis was then performed, and the fitted curves are presented in Fig. 8.

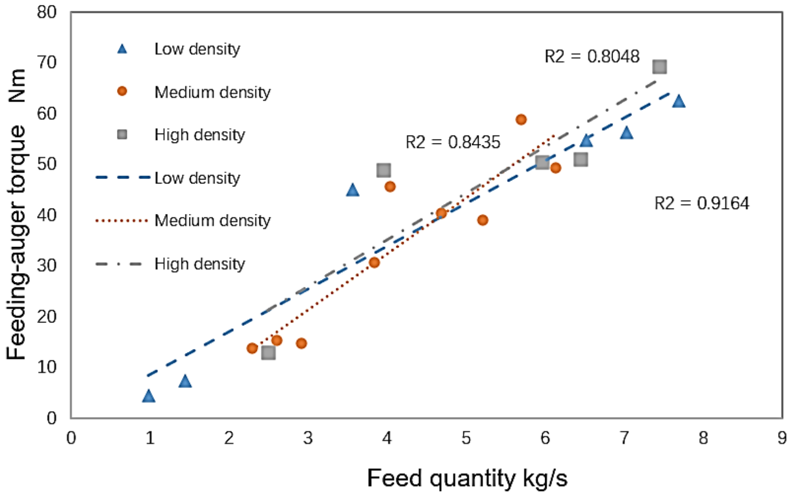

Fig. 8 - Regression curves relating feeding-auger torque to feed quantity under low-, medium-, and high-crop-density conditions

As shown in Fig. 8, feeding-auger torque exhibited a clear linear relationship with feed quantity under all three crop-density conditions. The strength of the relationship was highest under high-crop-density conditions, followed by medium- and low-crop-density conditions. The corresponding linear regression models are presented in Table 6.

Table 6

Linear regression models relating feeding-auger torque to feed quantity under different crop-density conditions

Crop-density level	Model form	Regression equation	Coefficient of determination
Low density	y=a x+b	y=22.102x+34.83	0.9628
Medium density	y=ax2+bx+c	y=1.3429x2+19.212x -6.7705	0.951
High density	y=a x+b	y=19.911x+34.83	0.9559

The analysis results indicated the presence of anomalous data points in the medium-crop-density dataset, which were attributed to irregular sensor measurements. After these anomalous points were removed, the remaining data exhibited a pronounced linear relationship between feeding-auger torque and feed quantity. Therefore, the valid samples obtained under medium-crop-density conditions were combined with those obtained under low-crop-density conditions for linear regression analysis. On this basis, the regression relationship for the medium-crop-density dataset was reconstructed, and the resulting fitted curve is presented in Fig. 9.

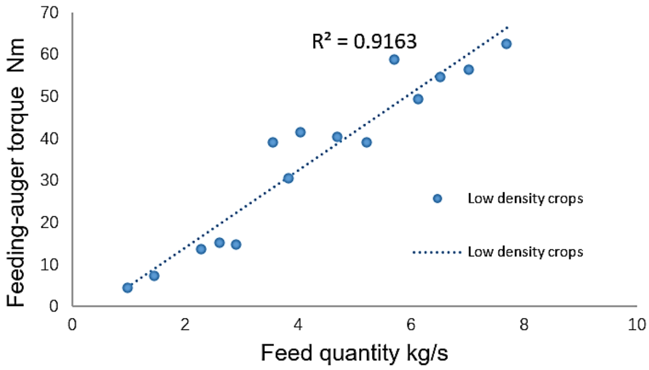

Fig. 9 - Regression relationship between feeding-auger torque and feed quantity under low-crop-density conditions

The data distribution for the high-crop-density condition was plotted, and regression analysis was performed. The resulting fitted curve is presented in Fig. 10.

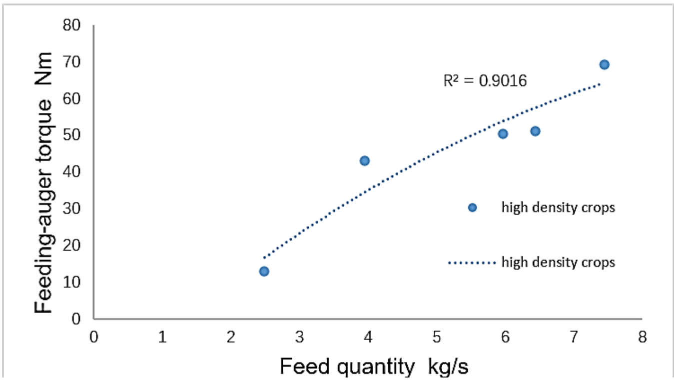

Fig. 10 - Regression relationship between feeding-auger torque and feed quantity under high-crop-density conditions

By comparing Figs. 9 and 10, it can be seen that different regression models were used to describe the relationship between feeding-auger torque and feed quantity under different crop-density conditions. A linear model was used for the combined low- and medium-crop-density data, whereas a quadratic model was used for the high-crop-density data. Both models exhibited relatively high coefficients of determination, indicating good fitting performance. In conclusion, the regression models describing the relationship between feed quantity and feeding-auger torque are presented in Table 7.

Table 7

Regression models relating feeding-auger torque to feed quantity under different crop-density conditions

Crop-density level	Model form	Regression equation	Coefficient of determination
Low and Medium density	y=a x+b	y = 9.1987x - 4.5299	0.9163
High density	y=ax2+bx+c	y=-0.7333x2+16.88x-20.796	0.9016

Analysis of the feed-quantity prediction model

During harvester operation, crop material passes through a series of conveying and processing stages. The wheat plants are first cut at the header and then enter the feeding auger, where they undergo initial compression before being transferred to the conveyor. The crop material is subsequently conveyed through the feeder house to the threshing drum, where threshing takes place. The straw is then separated and discharged, while the grain and impurities pass through the cleaning sieves. Finally, the cleaning system removes the remaining impurities and produces clean grain. Analysis of this material-flow process reveals a spatiotemporal delay between the feeding auger and the threshing drum during crop feeding. Consequently, the data collected from the different harvester components do not correspond to the same crop-material segment at the same instant and therefore cannot directly provide accurate real-time feedback on feed quantity for automatic harvester control.

To achieve spatiotemporal alignment between feed-quantity detection and the signals obtained from the feeding auger and threshing drum, and to reduce prediction delays caused by differences in material transport time, a model describing the crop-material conveying time through the harvester was established. The material-flow process is illustrated in Fig. 11.

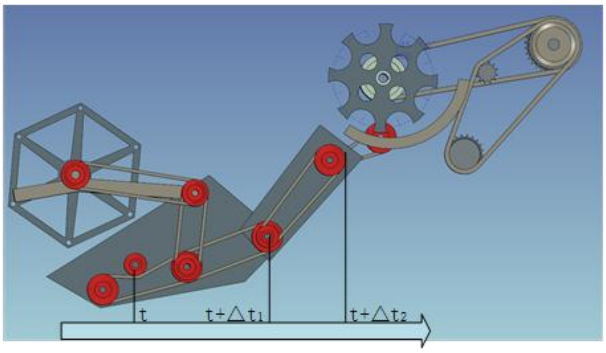

Fig. 11 - Crop-material conveying path through the combine harvester

As shown in Fig. 11, the crop-material conveying process begins when the crop enters the header and is subsequently transported from the feeding auger to the feeder house and then to the threshing drum. The transport time required for these two successive stages produces a delay in the crop-material flow. Neglecting frictional effects between the crop material and the conveying components, the time delay associated with crop transport from the feeding auger to the front end of the feeder house can be expressed by Eq. (1):

$$\Delta t_1 = \frac{L_1}{\omega_1 R_1} \tag{1}$$

where, L_1 is the effective conveying distance from the feeding auger to the front end of the feeder house, m; ω_1 is the rotational speed of the feeding auger, r/min; R_1 is the radius of the feeding-auger drive shaft, m.

The time delay associated with crop transport from the feeder house to the threshing drum was then analyzed and can be expressed by Eq. (2).

$$\Delta t_2 = \frac{L_2}{\omega_2 R_2} \tag{2}$$

where, L_2 is the effective conveying distance from the front end of the feeder house to the threshing drum, m; ω_2 is the rotational speed of the feeder-house conveyor drive shaft, r/min; R_2 is the radius of the feeder-house conveyor drive shaft, m.

Therefore, the total time delay required for the crop material to travel from the feeding auger to the threshing drum can be expressed by Eq. (3):

$$\Delta t = \Delta t_1 + \Delta t_2 = \frac{L_1}{\omega_1 R_1} + \frac{L_2}{\omega_2 R_2} = \frac{L_1 \omega_2 R_2 + L_2 \omega_1 R_1}{\omega_1 \omega_2 R_1 R_2} \tag{3}$$

Analysis of the crop-material transport delay from the header to the threshing drum indicates that, for a feed quantity $Q(t)$ entering the feeding system at time t, the corresponding operating parameters are the feeding-auger torque $T_1(t)$ and the threshing-drum torque $T_2(t + \Delta t_1 + \Delta t_2)$. The time shift in the threshing-drum torque signal results from the crop-material transport delays between the feeding auger, feeder house, and threshing drum.

By analyzing the relationships among key operating parameters, including feed quantity, operating speed, feeding-auger torque, and threshing-drum torque, this study determines the relative influence of each parameter and evaluates the time delay associated with the threshing-drum torque signal. On this basis, a multi-source information-fusion error-correction model based on relational weights is proposed for feed-quantity prediction. First, the pre-measured crop-density value is entered into the model. The real-time operating speed, feeding-auger torque, and threshing-drum torque are then integrated to obtain a preliminary estimate of feed quantity. Subsequently, the regression model relating threshing-drum torque to feed quantity is used to correct the error caused by the transport delay. The corrected value is then used as feedback to refine the preliminary prediction. After the correction is completed, the model proceeds to the next feed-quantity prediction cycle.

First, the initial feed-quantity prediction model is formulated as:

$$Q(t)=\varphi_1 Q_1(T_1(t))+\varphi_2 Q_v(v(t),\rho)+\Delta E(t) \tag{4}$$

where, φ_1 and φ_2 are the weighting coefficients of the prediction model, $Q(T_1)$ is the functional relationship between feed quantity and feeding-auger torque, $Q_v(v,\rho)$ is the functional relationship between feed quantity, operating speed, and crop density, $\Delta E(t)$ is the time-delay error-correction term.

The time-series error obtained from the current prediction cycle is used to correct the subsequent prediction, and the resulting correction term is denoted by $\Delta E(t)$.

First, the initial error sequence is defined as:

$$\Delta E^{(0)}(t)=\{e^{(0)}(t-nT),e^{(0)}(t-(n-1)T),e^{(0)}(t-(n-2)T),\cdots,e^{(0)}(t-(n-m)T),\cdots,e^{(0)}(t)\}$$

$$\begin{cases} n=1,2,3,\dots \\ m=1,2,3,\dots,n \end{cases} \tag{5}$$

where, T is the sampling interval of the threshing-drum torque signal. The sampling interval must be shorter than both transport-delay components, such that $T \le \Delta t_1$ and $T \le \Delta t_2$.

The elements of the initial error sequence are then expressed as:

$$\begin{aligned} e^{(0)}(t-(n-m)T)=\varphi_3(Q_2(T_2(t-(n-m)T))-Q(t-(n-m)\Delta t_1 T)) \\ -Q(t-(n-m)(\Delta t_1+\Delta t_2)T)) \end{aligned} \tag{6}$$

where, $Q_2(T_2)$ is the functional relationship between threshing-drum torque and feed quantity, and φ_1, φ_2 and φ_3 are the relational weighting coefficients corresponding to operating speed, feeding-auger torque, and threshing-drum torque, respectively.

By applying the accumulated generating operation to △E(0)(t), the following accumulated sequence is obtained:

$$\Delta E^{(1)}(t)=\left\{e^{(1)}(t-nT),e^{(1)}(t-(n-1)T),e^{(1)}(t-(n-2)T),\dots,e^{(1)}(t-(n-m)T),\dots,e^{(1)}(t)\right\}$$

$$e^{(1)}(t-(n-m)T)=\sum_{i=1}^{m}e^{(0)}(t-(n-i)T) \tag{7}$$

A first-order whitening differential equation is then established for the elements of the accumulated error sequence, as expressed in Eq. (8):

$$\frac{de^{(1)}}{dt}+ae^{(1)}=w \tag{8}$$

By discretizing Eq. 8, Eq. (9) is obtained:

$$\Delta^{(1)}(e^{(1)}(m+1))+az^{(1)}(e(m+1))=w \tag{9}$$

where, a and w are parameters to be determined.

The restored value of the sequence at time $m+1$ is then obtained by applying the inverse accumulated generating operation, as expressed in Eq. (10):

$$\Delta^{(1)}(e^{(1)}(m+1))=\Delta^{(0)}[e^{(1)}(m+1)]-\Delta^{(0)}[e^{(1)}(m)]=e^{(1)}(m+1)-e^{(1)}(m)=u^{(0)}(m+1)$$

$$z^{(1)}(e(m+1))=\frac{1}{2}(e^{(1)}(m+1)+e^{(1)}(m)) \tag{10}$$

Substituting Eq. (10) into Eq. (9) yields Eq. (11):

$$e^{(0)}(m+1)=a[-\frac{1}{2}(e^{(1)}(m)+e^{(1)}(m+1))]+w \tag{11}$$

By expanding Eq. (11) in series form, Eq. (12) is obtained:

$$\begin{bmatrix} e^{(0)}(2) \\ e^{(0)}(3) \\ . \\ . \\ . \\ e^{(0)}(m) \end{bmatrix} = \begin{bmatrix} -\frac{1}{2}(e^{(1)}(1)+e^{(1)}(2)) & 1 \\ -\frac{1}{2}(e^{(1)}(2)+e^{(1)}(3)) & 1 \\ . & . \\ . & . \\ . & . \\ -\frac{1}{2}(e^{(1)}(m-1)+e^{(1)}(m)) & 1 \end{bmatrix} \begin{bmatrix} a \\ w \end{bmatrix} \tag{12}$$

The auxiliary expressions are defined as follows:

$$Y = \begin{bmatrix} e^{(0)}(2) \\ e^{(0)}(3) \\ . \\ . \\ . \\ e^{(0)}(m) \end{bmatrix} \tag{13}$$

$$B = \begin{bmatrix} -\frac{1}{2}(e^{(1)}(1)+e^{(1)}(2)) & 1 \\ -\frac{1}{2}(e^{(1)}(2)+e^{(1)}(3)) & 1 \\ . & . \\ . & . \\ . & . \\ -\frac{1}{2}(e^{(1)}(m-1)+e^{(1)}(m)) & 1 \end{bmatrix} \tag{14}$$

$$\Phi = [a \quad w]^T \tag{15}$$

Substituting Eqs. (13)–(15) into Eq. (12) yields the corresponding sequence:

$$Y = B\Phi \tag{16}$$

The parameter vector Φ can then be estimated using the least-squares method, as expressed in Eq. (17):

$$\Phi = [a, w]^T = (B^T B)^{-1} B^T Y \tag{17}$$

Accordingly, the time-response sequence can be derived as:

$$\hat{e}^{(1)}(m+1) = [e^{(1)}(1) - \frac{w}{a}]e^{-am} + \frac{w}{a} \tag{18}$$

By substituting Eq. (11), the restored original sequence is obtained as follows:

$$\hat{e}^{(0)}(m+1) = \hat{e}^{(1)}(m+1) - \hat{e}^{(1)}(m) = (1-e^{a})[e^{(1)}(1) - \frac{w}{a}]e^{-am} \tag{19}$$

For the known weighting-coefficient vector $\phi=[\phi 1,\phi 2,\phi 3,\phi 4]$, the grey relational grade vector is defined as shown in Eq. (20):

$$\hat{e}^{(0)}(m+1) = \hat{e}^{(1)}(m+1) - \hat{e}^{(1)}(m) = (1-e^{a})[e^{(1)}(1) - \frac{w}{a}]e^{-am} \tag{20}$$

The weighting coefficients corresponding to operating speed, feeding-auger torque, threshing-drum torque, and the fourth model parameter can then be determined as follows:

$$\varphi_k = \frac{\gamma_i}{\sum_{k=1}^{k=i} \gamma_k} \tag{21}$$

Experimental validation of the feed-quantity prediction model

The experiment was conducted at the wheat-growing base of Shengfa Cooperative in Jimo District, Qingdao. A modified GM-series combine harvester manufactured by Lovol was used, and the tested wheat cultivar was Jinan No. 17. Before the field tests, samples were collected from the experimental plot to determine key crop characteristics, including crop density and grain moisture content.

During each test, the harvester operated at a constant forward speed, while the crop material was fed manually to determine the actual feed quantity for the corresponding test plot. A total of 12 tests were conducted, and the validation results are presented in Table 8.

Table 8

Validation results for the feed-quantity prediction model

No.	Predicted feed quantity (kg/s)	Measured feed quantity (kg/s)	Absolute error	Relative error (%)
1	0.91	0.83	0.08	9.64
2	3.88	3.75	0.13	3.47
3	4.09	4.28	-0.19	4.44
4	1.5	1.65	-0.15	9.09
5	5.01	4.89	0.12	2.45
6	5.18	5.26	-0.08	1.52
7	3.38	3.16	0.22	6.96
8	5.72	5.9	-0.18	3.05
9	6.44	6.33	0.11	1.74
10	5.29	5.34	-0.05	0.94

After excluding the data from Tests 11 and 12, the maximum absolute error among the remaining samples was 0.22 kg/s, the maximum relative error was 9.64%, and the mean relative error was 4.33%. All relative errors were below 10%, indicating that the prediction model satisfied the specified measurement-error requirements.

In conclusion, the accuracy of detection and errors of the prediction model differ based on various feeding conditions. To analyze the variances in the feed quantity prediction models at different stages, the test data samples are divided into regions of low feed quantity, medium feed quantity, and high feed quantity. A comparative column chart is depicted in Fig. 12 to illustrate the differences.

Overall, the prediction accuracy and error varied under different feeding conditions. To evaluate the performance of the feed-quantity prediction model across different operating ranges, the validation samples were divided into low-, medium-, and high-feed-quantity groups. A comparative bar chart illustrating the prediction results and errors for these three groups is presented in Fig. 12.

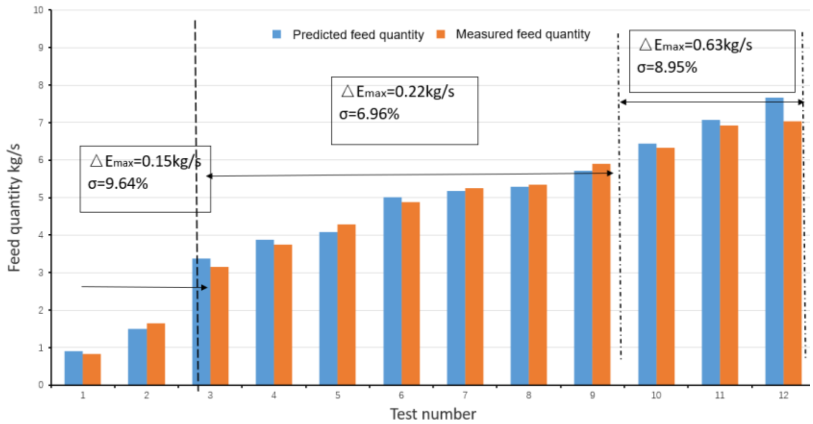

Fig. 12 - Comparison of measured and predicted feed quantities across different feed-quantity ranges

As shown in Fig. 12, the feed-quantity range was divided into three intervals: 0-3 kg/s, 3-6 kg/s, and 6-8 kg/s. The maximum relative errors in these intervals were 9.64%, 6.96%, and 8.95%, respectively. Comparison of the prediction results indicates that the model produced larger errors at low and high feed quantities, whereas its prediction performance was more accurate within the medium feed-quantity range.

CONCLUSIONS

(1) Grey relational weight analysis was used to determine the relative influence of the main operating parameters on feed quantity. Harvester operating speed had the highest relational weight (0.89), followed by feeding-auger torque (0.84) and threshing-drum torque (0.72). These results indicate that variations in feed quantity are primarily governed by changes in operating speed, whereas variations in feeding-auger and threshing-drum torque reflect the dynamic relationship between crop intake, material conveying, and threshing load.

(2) A piecewise modelling approach was adopted for different crop-density conditions. Under low- and high-crop-density conditions, feed quantity exhibited a strong linear relationship with threshing-drum torque, with coefficients of determination of R^2 = 0.9628 and 0.9559, respectively. Under medium-crop-density conditions, a quadratic model provided a better fit, with R^2 = 0.951. This result suggests that crop-flow and separation processes within the threshing system become more complex under medium-crop-density conditions and cannot be adequately described using a simple linear relationship.

(3) To compensate for the time delay in the signals collected from different harvester components, an error-corrected feed-quantity prediction model was developed. Field-validation results showed that, across the 12 test groups, the maximum absolute error was 0.63 kg/s, the maximum relative error was 9.64%, and the mean relative error was 4.55%. Further analysis by feed-quantity range showed that the maximum relative errors for the low (0–3 kg/s), medium (3–6 kg/s), and high (6–8 kg/s) ranges were 9.64%, 6.96%, and 8.95%, respectively. The model achieved the highest prediction accuracy within the medium feed-quantity range, whereas larger errors occurred at low and high feed quantities. These differences may be attributed to weaker sensor signals and a lower signal-to-noise ratio under low-feed conditions, as well as increased crop accumulation and greater torque fluctuations under high-feed conditions.

ACKNOWLEDGEMENT

This work was supported by the Opening Fund of State Key Laboratory of Agricultural Equipment Technology (SKL2025006); Doctoral Research Startup Fund Project of Weifang University(2024BS38)

REFERENCES

[1] Abdeen, M. A. M., Xie, G., Salem, A. E., Fu, J., & Zhang, G. (2022). Longitudinal axial flow rice thresher feeding rate monitoring based on force sensing resistors. *Scientific Reports*, Vol. 12, 1369, United Kingdom.

[2] Chen, D., & Wang, S. M. (2019). Design and Test of Feed Rate Monitoring System for Combine Harvester (联合收割机喂入量监测系统设计与试验). *Transactions of the Chinese Society for Agricultural Machinery*, Vol. 50, No. 6, pp. 85-92, China.

[3] Chen, X., Wu, S., Li, C., Liu, F., Yuan, L., & Wang, W. (2025). Design and experiment of feed rate monitoring system based on the action force of grain combine harvester reel. *Computers and Electronics in Agriculture*, Vol. 228, 109837, Netherlands.

[4] Ebrahimi-Nik, M., Khademolhosseini, N., Abbaspour-Fard, M. H., Mahdinia, A., & Alami-Saied, K. (2009). Optimum utilisation of low-capacity combine harvesters in high-yielding wheat farms using multi-criteria decision making. *Biosystems Engineering*, Vol. 103, No. 3, pp. 382-388, United Kingdom.

[5] Fricke, T., Richter, F., & Wachendorf, M. (2011). Assessment of forage mass from grassland swards by height measurement using an ultrasonic sensor. *Computers and Electronics in Agriculture*, Vol. 79, No. 2, pp. 142-152, Netherlands.

[6] Jiang, L., Wang, G., Xu, B., Husnain, N., & Wang, Q. (2025). Intelligent Systems for Combine Harvesters: A Comprehensive Review of Technologies and Trends. *IEEE Transactions on Industrial Informatics*, Vol.21, No. 12, pp. 1-15, United States.

[7] Li, Q., Yu, Y., Guo, G., Hu, J., Liu, P., Chai, X., Wang, Y., & Xu, L. (2024). Design and experiment of array-based fingerplate differential flow sensor for rice grain monitoring. *INMATEH - Agricultural Engineering*, Vol. 74, No. 3, pp. 358-369, Romania.

[8] Li, X. H., Qiu, Z. P., Jiang, J. C., Zhang, Y., Xing, C. X., & Wu, X. (2026). Magnetoelastomer-based grain flow sensor for combine harvesters. *Computers and Electronics in Agriculture*, Vol. 244, 111447, Netherlands.

[9] Liang, Z., Qin, Y., & Su, Z. (2024). Establishment of a Feeding Rate Prediction Model for Combine Harvesters. Agriculture, Vol. 14, No. 4, 589, Switzerland.

[10] Liu, A., Li, P., Xie, F., Zeng, L., & Ji, B. (2026). A feed rate monitoring system based on light loss in the conveyor trough of soybean combine harvester. *Computers and Electronics in Agriculture*, Vol. 238, 111005, Netherlands.

[11] Mathanker, S. K., Buss, J. C., Gan, H., Larsen, J. F., & Hansen, A. C. (2015). Stem bending force and hydraulic system pressure sensing for predicting napiergrass yield during harvesting. *Computers and Electronics in Agriculture*, Vol. 111, pp. 174-180, Netherlands.

[12] Saeys, W., Lenaerts, B., Craessaerts, G., & De Baerdemaeker, J. (2009). Estimation of the crop density of small grains using LIDAR sensors. *Biosystems Engineering*, Vol. 102, No. 1, pp. 22-30, United Kingdom.

[13] Sangeetha, C., Moond, V., Rajesh G. M., Damor, J. S., Pandey, S. K., Kumar, P., & Singh, B. (2024). Remote Sensing and Geographic Information Systems for Precision Agriculture: A Review. *International Journal of Environment and Climate Change*, Vol. 14, No. 2, pp. 287-309, India.

[14] Sun, Y., Liu, R., Zhang, M., Li, M., Zhang, Z., & Li, H. (2022). Design of feed rate monitoring system and estimation method for yield distribution information on combine harvester. *Computers and Electronics in Agriculture*, Vol. 201, 107322, Netherlands.

[15] Wang, F., Chen, L. P., Wang, Q., Qin, W. C., & Meng, Z. J. (2026). Design and experimental validation of a flow-guided weighing-based grain mass flow sensor for wheat combine harvester. *Computers and Electronics in Agriculture*, Vol. 240, 111224, Netherlands.

[16] Wang, J., Fang, X., Wang, F., Liu, Y., & Zhao, B. (2023). Study on the loss control system of wheat combine harvester. *INMATEH - Agricultural Engineering*, Vol. 69, No. 1, pp. 471-480, Romania.

[17] Wang, Q., Yin, Y., Meng, Z., Qin, W., & Geng, D. (2026). Research on Feeding Rate Measurement Method for Combine Harvester Based on Multimodal Information Fusion. *IEEE Journal of Selected Topics in Signal Processing*, Vol. 20, No. 2, pp. 115-128, United States.

[18] Yang, X., Li, P., Zhao, Z., Lei, C., & Jin, C. (2025). A review of the feed rate detection and stability control methods in combine harvesters. *INMATEH - Agricultural Engineering*, Vol. 75, No. 1, pp. 143-157, Romania.

[19] Zhang, C., Li, Q., Ye, S., & Zheng, D. (2025). Design and test of a wireless monitoring system for feed rate in combine harvester based on bottom plate pressure of chain-rake conveyor. *INMATEH - Agricultural Engineering*, Vol. 77, No. 3, pp. 894-903, Romania.

[20] Zhang, Y., Yin, Y., Meng, Z., Chen, D., Qin, W., Wang, Q., & Dai, D. (2022). Development and testing of a grain combine harvester throughput monitoring system. *Computers and Electronics in Agriculture*, Vol. 200, 107253, Netherlands.

[21] Zhang, Y., Zhang, B., Shen, C., Liu, H., Huang, J., Tian, K., & Tang, Z. (2024). Review of the field environmental sensing methods based on multi-sensor information fusion technology. International *Journal of Agricultural and Biological Engineering*, Vol. 17, No. 2, pp. 1-13, United States.